ChemComm

Accepted Manuscript

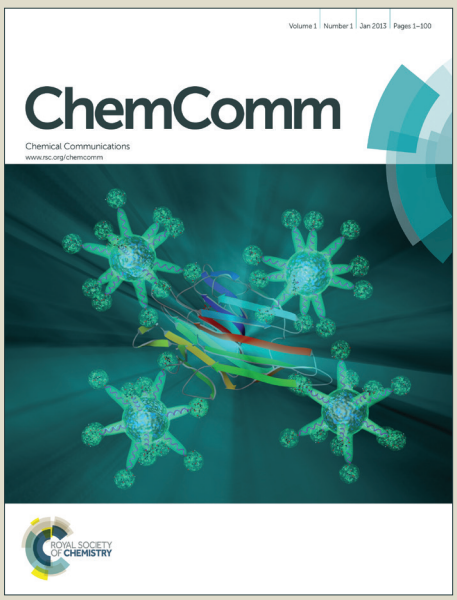

ROYAL SOCIETY OF CHEMISTRY

www.rsc.org/chemcomm

Journal Name

RSCPublishing

COMMUNICATION

Modulating H_2 Sorption in Metal-organic Frameworks via Ordered Functional Groups†

Cite this: DOI: 10.1039/x0xx00000x

Phuong V. Dau[a] and Seth M. Cohen[a]*

Received ooth January 2012,
Accepted ooth January 2012

DOI: 10.1039/x0xx00000x

www.rsc.org/

Herein, we present the use of presynthetic and postsynthetic modification (PSM) approaches to regulate the structural organization of functional groups in the pores of isoreticular metal-organic frameworks (IRMOFs). It has been found that the structural ordering of aryl groups within the IRMOF pores results in hysteretic H_2 sorption, while the same aryl groups introduced in a disordered manner displays reversible H_2 sorption that is more typical of the IRMOF family.

Metal-organic frameworks (MOFs) are an increasingly popular class of porous materials that have been investigated for applications such as gas storage,[1] separation,[2] and catalysis.[3] The advantages of MOFs in comparison with other porous materials (e.g. activated carbon, zeolites, and silica) includes functional tunability, controllable pore-sized, and a highly ordered structure.[4] Because of these features, as well as their very high surface areas and fast kinetics of gas sorption/desorption, MOFs have been extensively investigated for H_2 storage. H_2 is among one of the most promising candidates for the replacement of current carbon-based energy resources.[1] However, the use and application of hydrogen as a clean alternative to fossil fuels is limited, in part, due to the lack of a convenient, safe, and cheap storage system. While the H_2 sorption of MOFs displays excellent reversibility and fast kinetics, due to its high internal porosity, the weak dispersive interactions between H_2 and the MOF typically result in the need to employ low operating temperatures and high pressures to achieve an acceptable storage capacity.[1]

In the past decade, several strategies have been employed to increase interactions between H_2 and MOFs such as narrow pore sizes,[5, 6] structural flexibility,[7-11] and unsaturated metal sites.[12-15] Recently, kinetic trapping of H_2 in MOFs has been exploited to enhance H_2 uptake. This approach improves gas storage by confining H_2 within the framework at high pressure and not allowing it to be as easily released upon a reduction in pressure. Hysteresis is typically achieved via structural flexibility of certain MOFs (i.e. 'breathing') or by the use of gating substituents that favor access, but restrict release of guest molecules.[16] These are effective approaches, but can be limited by the ability to rationally design flexible MOFs or predict the gating behaviour of substituents.[17, 18]

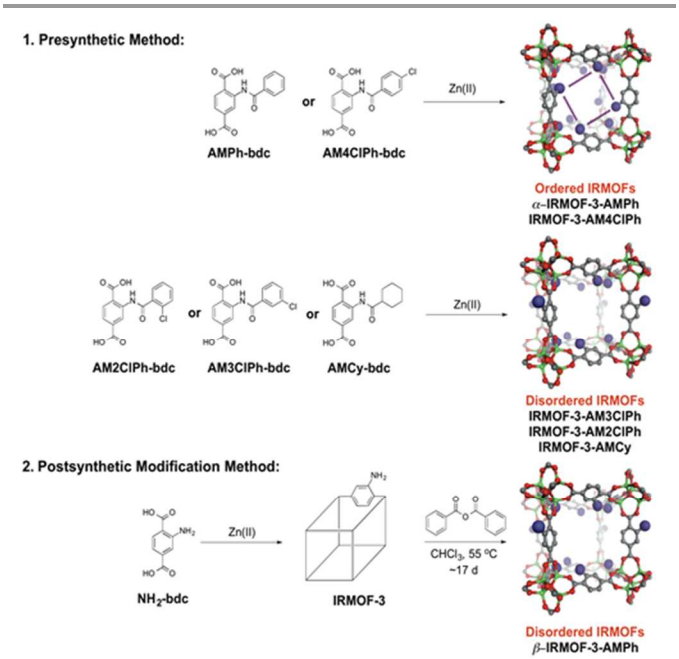

Figure 1. The synthesis of IRMOFs with ordered and disordered substituents using pre- and post-synthetic methods.

A strategy for modulating gas sorption that has not been widely reported is via the organization and distribution of functional groups within MOFs. This is a substantial challenge due to the difficulty in both preparing,[19] but also unambiguously determining the organization and distribution of functional groups within a MOF.[20, 21] Herein, we present the first study to report the formation of identical isoreticular MOFs (IRMOFs) that possess either ordered, well-organized functional groups within the pores or a dissordered arrangement of the same pendant groups.[22] Order versus disorder

was achieved via employing pre- and post-synthetic methods, respectively (Fig. 1). Importantly, it is found that IRMOFs with ordered aryl substituents display hysteretic H_2 sorption, while those with disordered aryl substituents display non-hysteretic, fully reversible H_2 sorption.

Previously, it was reported that postsynthetic modification (PSM) could partially convert IRMOF-3, which uses 2-amino-1,4-benzene dicarboxylate (NH_2-bdc) as a linker, to IRMOF-3-AMPh (70% conversion), which has a phenylamide substituent attached to the dicarboxylate linker (Fig. 1).[5] Despite incomplete conversion, IRMOF-3-AMPh showed improved H_2 uptake capacity and heat of adsorption.[5] In an attempt to produce IRMOF-3-AMPh with only AMPh-bdc ligands (i.e. 100% conversion), a presynthetic method was used to prepare this IRMOF (Fig. 1). The synthesis of the ligand (AMPh-bdc) was easily achieved in high yield via a two-step synthesis (Fig. S1 and S2). The combination of Zn(II) and AMPh-bdc under solvothermal conditions yielded clear square blocks of *α*-IRMOF-3-AMPh. ^{1}H NMR digestion of *α*-IRMOF-3-AMPh showed that the phenylamide substituents remained intact under the standard solvothermal conditions for IRMOFs (Fig. S4). Thermal gravimetric analysis (TGA) revealed that *α*-IRMOF-3-AMPh possessed thermal stability comparable to other IRMOF derivatives (Fig. S5). Single-crystal X-ray diffraction (XRD) analysis of *α*-IRMOF-3-AMPh showed the framework occupied a cubic *P* crystal system rather than typical cubic *F* crystal system found for most IRMOFs. The lower symmetry of *α*-IRMOF-3-AMPh was revealed to be a consequence of an ordered isomer of this IRMOF, in which the pendant phenyl substituents are highly ordered and can be readily located and refined from the XRD data (Fig. 2). The ordered structure of *α*-IRMOF-3-AMPh was confirmed by collecting multiple data sets from several independent batches of *α*-IRMOF-3-AMPh crystals.

α-IRMOF-3-AMPh possesses the typical Zn_4O secondary building units (SBUs) connected by AMPh-bdc linkers to form the IRMOF topology (Fig. 2). However, unlike other functionalized IRMOFs, the phenylamide substituent is highly ordered and exhibits intermolecular edge-to-face interactions (~4.0 Å) with adjacent linkers (Fig. 2). Hence, the pores of *α*-IRMOF-3-AMPh are symmetrically decorated with phenyl groups throughout the framework lattice (Fig. S6). This ordering results in an arrangement where each cubic unit of *α*-IRMOF-3-AMPh is either occupied by six phenylamide substituents or none (Fig. S6). These two types of cubic units pack in an alternating fashion in the overall infinite structure of *α*-IRMOF-3-AMPh (Fig. S6). The unexpected organization of the phenylamide groups within *α*-IRMOF-3-AMPh likely originates from the intermolecular π-π edge-to-face interactions and forms via self-assembly during the solvothermal synthesis.[23] The ordered *α*-IRMOF-3-AMPh is the first example to use intermolecular interactions between functional groups to prevent the typical disordered of such groups within the highly symmetric IRMOF lattice.

The distribution and position of the functional groups within the lattice of MOFs have been theoretically and experimentally showed to have significant influences on gas sorption properties.[17, 21] Therefore, to enable a comparative study, a disordered isomer of IRMOF-3-AMPh was desired. A PSM approach was selected to obtain the desired compound.[24] First, IRMOF-3 was prepared, which contains the expected, positionally disordered amino substituents within the framework. Using more forcing conditions then our previous report,[5] IRMOF-3 was then completely converted into *β*-IRMOF-3-AMPh by incubating reaction with benzoic anhydride. ^{1}H NMR and mass spectrometry (MS) analysis confirmed full (~99%) conversion of NH_2-bdc to AMPh-bdc (Fig. S7 and S8). As expected, both single-crystal XRD and powder X-ray diffraction (PXRD) analysis of *β*-IRMOF-3-AMPh reveal a typical, disordered IRMOF structure (cubic *F*, Fig. S9). As anticipated, the disordered isomer is obtained from the disorder of the amine groups in the IRMOF-3 precursor. In addition, attempts to solve and refine the structure of *β*-IRMOF-3-AMPh with lower symmetry system (cubic *P*) reveal the same disordered IRMOF structure.

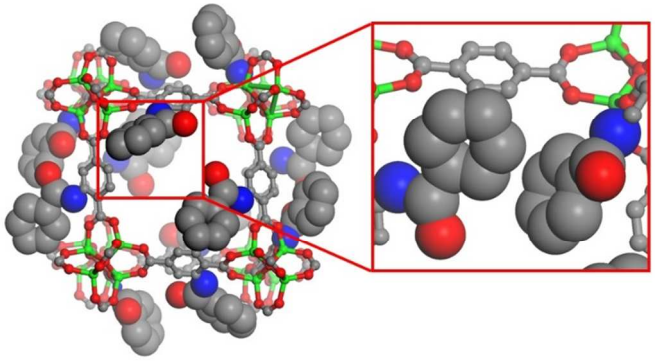

Figure 2. Crystal structure of ordered *α*-IRMOF-3-AMPh (left). *α*-IRMOF-3-AMPh with ordered phenylamide groups, highlighting intermolecular edge-to-face interactions between these substituents (right). Color scheme: carbon (grey), nitrogen (blue), oxygen (red), and zinc (green). Hydrogen atoms were omitted for clarity.

The influence of the shape and composition of the aromatic group on the ability to form ordered IRMOF structures was also investigated. Chloro-substituted derivatives were prepared (Fig. S1 and S2) and in combination with Zn(II) under standard solvothermal conditions produced cubic crystals (Fig. 1). Single-crystal XRD analysis of IRMOF-3-AM4ClPh reveals an ordered, cubic IRMOF structure (cubic *P*, Fig. 3, and S10), while both IRMOF-3-AM3ClPh and IRMOF-3-AM2ClPh possess the more typical disordered IRMOF structure (cubic *F*, Fig. S11). The structure of IRMOF-3-AM4ClPh shows similar edge-to-face interactions (~4.0 Å) with phenylamide groups of adjacent ligands, with the chlorine atom occupying open space within the framework (Fig. 3, S10). IRMOF-3-AM4ClPh has an identical alternating arrangement of cubic units as in *α*-IRMOF-3-AMPh (Fig. S4). Based on these results, it appears that the chlorine atoms of AM2ClPh-bdc and AM3ClPh-bdc interfere with the self-assembly of ordered phases (Fig. S10 and S11).

To verify the contribution of the intermolecular π-π edge-to-face interactions in the formation of ordered IRMOF derivatives, AMCy-bdc (containing a cyclohexyl substituent) was synthesized and incorporated into the IRMOF structure via a presynthetic method (Figure S3). As expected, the cubic lattice of IRMOF-3-AMCy reveals a disordered structure (Cubic *F*, Fig. S12). Hence, the shape and intermolecular interactions between functional groups must play a role in the generation of ordered versus disordered structural isomers.

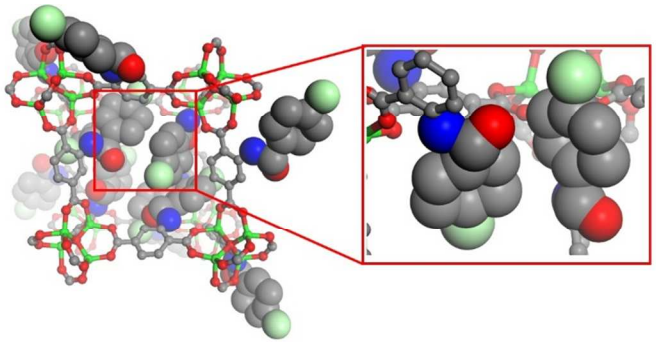

Figure 3. Crystal structure of IRMOF-3-AM4ClPh (left). IRMOF-3-AM4ClPh with ordered 4-chlorophenylamide groups, highlighting intermolecular edge-to-face interactions between substituents (right). Color scheme: carbon (grey), chlorine (light green), nitrogen (blue), oxygen (red), and zinc (green). Hydrogen atoms were omitted for clarity.

PXRD analysis of this series of IRMOFs reveals similar patterns (Fig. 4 and S13). Notably, experimental PXRD patterns of *α*-IRMOF-3-AMPh and IRMOF-3-AM4ClPh have a weak reflection at low angle (2θ = ~6°) that is not observed in experimental patterns of IRMOFs with disordered substituents. This observed reflection is due to the crystallographic (1 1 1) plane, which lies on the ligand in the unit cell of both *α*-IRMOF-3-AMPh and *β*-IRMOF-3-AMPh. We therefore attribute observation of reflection in α-IRMOF-3-AMPh and IRMOF-3-AM4ClPh, but not the other MOFs reported here (or more generally other IRMOFs), to the ordered substituents in these structures. Reflection intensity can vary with localization of the electron density (Fig. 4, S13), hence explaining the increased intensity of this reflection in these more ordered structures. Overall, the PXRD patterns of ordered IRMOFs shows this reflection, as predicted by simulation, while PXRD patterns of disordered IRMOFs show no evidence of this reflection at low angle, thereby supporting the difference in the single-crystal XRD analysis of these materials (Fig. S13).

To explore the effect of substituent ordering on framework properties, a series of gas uptake studies were performed after MOFs had been fully activated. Complete activation was evidenced by ^{1}H NMR digestion and TGA, both of which were indicative of guest-free materials (Fig. S4 and S5). Brunauer-Emmett-Teller (BET) surface areas of *α*-IRMOF-3-AMPh and *β*-IRMOF-3-AMPh were determined to be 7±6 m^2 g^{-1} and 1521±28 m^2 g^{-1} under identical activation conditions, respectively. Amazingly, the ordered, uniform distribution of the aryl functional groups within pores exhibits a pronounced effect of surface area consistent with prior studies.[21] The void spaces of *α*-IRMOF-3-AMPh and *β*-IRMOF-3-AMPh were calculated from the X-ray structures (using PLATON)[25] to be 9011 $Å^3$ and 11867 $Å^3$ per unit cell, respectively. Because the calculated void spaces are similar for these MOF isomers, this suggests that the low porosity observed for N_2 with *α*-IRMOF-3-AMPh (kinetic radius ~3.64 Å) may be due to hindered diffusion into *α*-IRMOF-3-AMPh due to the close, ordered packing of the functional groups (Fig. S6). Despite being isomers, the porosity of *α*- and *β*-IRMOF-3-AMPh to N_2 are very distinct, indicating a substantial influence originating from the substituent organization.

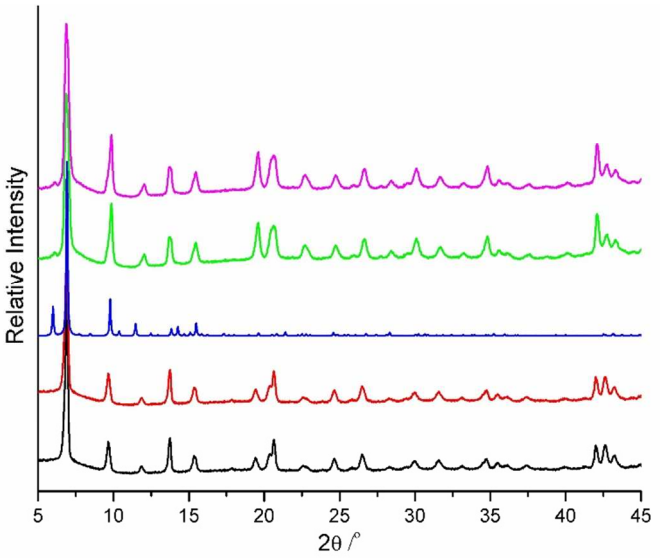

Figure 4. PXRD analysis of IRMOF-3 (black), *β*-IRMOF-3-AMPh (red), simulated *α*-IRMOF-3-AMPh (blue), *α*-IRMOF-3-AMPh (green), and IRMOF-3-AM4ClPh (magenta).

To further explore this interesting phenomenon, the sorption of these IRMOFs was studied with H_2 (kinetic radius = 2.89 Å). While *β*-IRMOF-3-AMPh displays a typical reversible H_2 sorption isotherm at 77 K, *α*-IRMOF-3-AMPh displays a marked hysteresis in the same isotherm (Fig. 5, S14). Remarkably, the H_2 desorption of ordered *α*-IRMOF-3-AMPh shows the frameworks restrict the release of H_2 at high pressure (from 810 down to ~100 mmHg), followed by rapid desorption of the H_2 at lower pressure (<100 mmHg). Even approaching ~0 mmHg, approximate 25% of the overall H_2 uptake capacity of *α*-IRMOF-3-AMPh remains trapped in the framework, indicating the framework can kinetically trapped H_2 molecules at low pressure.[10, 12, 16] Similarly, ordered IRMOF-3-AM4ClPh displays hysteretic H_2 sorption (Fig. S15). In contrast, disordered IRMOF-3-AM3ClPh, IRMOF-3-AM2ClPh, and IRMOF-3-AMCy show non-hysteretic H_2 sorption isotherms at 77 K (Fig. S14). These results all indicate that the origin of hysteretic H_2 sorption of *α*-IRMOF-3-AMPh originates from the ordered and uniformed distribution of functional groups within the pores through an apparent gating effect.

Conclusions

Together, these results describe a self-assembly process that results in the ordering of functional groups in the pores of IRMOFs, providing access to ordered and disordered IRMOF structural isomers. While kinetic H_2 trapping has been reported in MOFs with either structural flexibility or that contain unsaturated metal sites, the results here present the first report to use self-assembly resulting structural organization to induce similar effects. The fast uptake and hindered release kinetics of H_2 in these ordered IRMOFs suggest that functionalization of MOFs can be used to further improve gas sorption performance of MOFs for applications in H_2 storage via gating. While the ordered IRMOFs display H_2 trapping, the overall H_2 uptake capacity of these IRMOFs (α-IRMOF-3-AMPh ~35 cm^3 g^{-1} and

IRMOF-3-AM4ClPh ~50 cm^3 g-1 at 77 K and ~800 mmHg) is notably decreased with respect to the parent IRMOF-1 (510 cm^3 g^{-1} at 78 K and ~800 mmHg)[26] and IRMOF-3 (~170 cm^3 g^{-1} at 77 K and ~800 mmHg).[5] Efforts are now underway to design core-shell IRMOF materials that combine a high capacity core material with an outer-shell of material with gating functional groups. Such a MOF could combine the best of both materials to produce a construct ideal for H_2 storage.

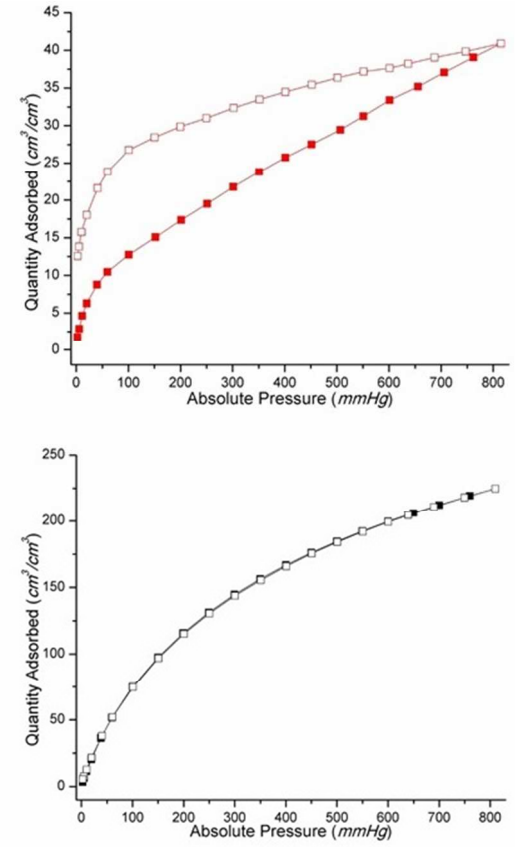

Figure 5. H_2 sorption isotherms at 77 K of α-IRMOF-3-AMPh (red, top) and β-IRMOF-3-AMPh (black, bottom). Filled symbols represent adsorption process, and emptied symbols represent desorption process.

We thank the UCSD Small Molecule Mass Spectrometry and X-ray diffraction facilities for assistance with experiments. This work was supported by a grant from the Department of Energy, Office of Basic Energy Sciences, Division of Materials Science and Engineering under Award No. DE-FG02-08ER46519.

Notes and references

[a] Department of Chemistry and Biochemistry, University of California, San Diego, La Jolla, USA 92093. Email: scohen@ucsd.edu. Tel: 1-858-522-5596.

† Electronic Supplementary Information (ESI) available: Ligands, MOFs characterization and crystallographic tables. Crystal structures of MOFs are deposited into Cambridge Structural Database (CCDC-987960-987965). See DOI: 10.1039/b000000x/

1. M. P. Suh, H. J. Park, T. K. Prasad and D.-W. Lim, *Chem. Rev.*, 2012, **112**, 782-835.
2. J.-R. Li, J. Sculley and H.-C. Zhou, *Chem. Rev.*, 2012, **112**, 869-932.
3. M. Yoon, R. Srirambalaji and K. Kim, *Chem. Rev,*, 2012, **112**, 1196-1231.
4. M. O'Keeffe and O. M. Yaghi, *Chem. Rev.*, 2012, **112**, 675-702.
5. Z. Wang, K. K. Tanabe and S. M. Cohen, *Chem. Eur. J.*, 2010, **16**, 212-217.
6. L. J. Murray, M. Dincă and J. R. Long, *Chem. Soc. Rev.*, 2009, **38**, 1294-1314.
7. H. J. Choi, M. Dincă and J. R. Long, *J. Am. Chem. Soc.*, 2008, **130**, 7848-7850.
8. J. Kang, S.-H. Wei and Y.-H. Kim, *J. Am. Chem. Soc.*, 2010, **132**, 1510-1511.
9. H. J. Choi, M. Dincă, A. Dailly and J. R. Long, *Energy Environ. Sci.*, 2010, **3**, 117-123.
10. X. Zhao, B. Xiao, A. Fletcher, K. M. Thomas, D. Bradshaw and M. J. Rosseinsky, *Science*, 2004, **306**, 1012-1015.
11. D.-C. Zhong, W.-X. Zhang, F.-L. Cao, L. Jiang and T.-B. Lu, *Chem. Comm.*, 2011, **47**, 1204-1206.
12. S. Yang, X. Lin, A. J. Blake, G. S. Walker, P. Hubberstey, N. R. Champness and M. Schröder, *Nature Chemistry*, 2009, **1**, 487-493.
13. K. Sumida, D. Stuck, L. Mino, J.-D. Chai, E. D. Bloch, O. Zavorotynska, L. J. Murray, M. Dincă, S. Chavan, S. Bordiga, M. Head-Gordon and J. R. Long, *J. Am. Chem. Soc.*, 2013, **135**, 1083-1091.
14. M. Dincă and J. R. Long, *Angew. Chem. Int. Ed.*, 2008, **47**, 6766-6779.
15. K. Sumida, C. M. Brown, Z. R. Herm, S. Chavan, S. Bordiga and J. R. Long, *Chem. Comm.*, 2011, **47**, 1157-1159.
16. Y. Sihai, S. K. Callear, A. J. Ramirez-Cuesta, W. I. F. David, J. Sun, A. J. Blake, N. R. Champness and M. Schröder, *Farraday Discussions*, 2011, **151**, 19-36.
17. M. Kim, J. A. Boissonnault, P. V. Dau and S. M. Cohen, *Angew. Chem. Int. Ed.*, 2011, **50**, 12193-12196.
18. S. Henke, A. Schneemann, A. Wutscher and R. A. Fischer, *J. Am. Chem. Soc.*, 2012, **134**, 9464-9474.
19. L. Liu, K. Konstas, M. R. Hill and S. G. Telfer, *J. Am. Chem. Soc.*, 2013, **135**, 17731-17734.
20. P. V. Dau, M. Kim and S. M. Cohen, *Chem. Sci.*, 2013, 601-605.
21. X. Kong, H. Deng, F. Yan, J. Kim, J. A. Swisher, B. Smit, O. M. Yaghi and J. A. Reimer, *Science*, 2013, **341**, 882-885.
22. H. Yim, E. Kang and K. J., *Bull. Korean Chem. Soc.*, 2010, **31**, 1041-1042.
23. E. G. Hohenstein and C. D. Sherrill, *J. Phys. Chem. A*, 2009, **113**, 878-886.
24. S. M. Cohen, *Chem. Rev.*, 2012, **112**, 970-1000.
25. A. L. Spek, *Acta Cryst.*, 2009, **D65**, 148-155.
26. N. L. Rosi, J. Eckert, M. Eddaoudi, D. Vodak, J. Kim, M. O'Keeffe and O. M. Yaghi, *Science*, 2003, **300**, 1127-1129.

